Available online at www.sciencedirect.com

SCIENCE DIRECT®

Catalysis Today 113 (2006) 187–193

CATALYSIS TODAY

www.elsevier.com/locate/cattod

Ni catalysts from $NiAl_2O_4$ spinel for CO_2 reforming of methane

N. Sahli [a,c], C. Petit [a,*], A.C. Roger [a], A. Kiennemann [a], S. Libs [a], M.M. Bettahar [b]

[a] *Ecole Européenne de Chimie, Polymères et Matériaux de Strasbourg-Laboratoire Matériaux, Surface, Procédés Pour la Catalyse UMR 7515-25 Rue Becquerel 67087 Strasbourg Cedex 2, France*

[b] *Equipe de Recherche Réactivité et Synthèse Organique, Groupe Catalyse Hétérogène-UMR 7565-Université H. Poincaré, Nancy-1 BP 239 54506 Vandoeuvre-les-Nancy Cedex, France*

[c] *Laboratoire de Chimie du Gaz Naturel, Faculté de Chimie, USTHB 109 El-Alia Bab Ezzouar Alger, Algerie*

Abstract

A series of mixed oxides close to $NiAl_2O_4$ was obtained by a sol–gel like method (propionic acid). The characterization of the different structures was made by X-ray diffraction (XRD), scanning electron microscopy (SEM) or transmission electron microscopy (TEM). For the stoichiometric ratio of Ni to Al exactly equal to 0.5, homogeneous crystalline spinel phase was formed for a temperature of calcination equal or higher than 725 °C. A solid solution was obtained for a Ni/Al ratio lower than 0.5. The spinel structure is non-tolerant concerning a change of nickel to aluminum ratio higher than 0.5: an excess of nickel gives large particles of NiO on spinel phase. Comparative reduction and dry reforming of these oxides was made to control the formation of Ni and its sintering for applications in methane dry reforming. Preliminary reactivity results in dry reforming of methane are given.

Keywords: Spinel; Catalyst; Nickel; Syngas

1. Introduction

Increasing attention from both academic and industrial areas has been paid to the dry reforming of methane to produce synthesis gas of low H_2/CO ratios [1,2]. However, the strong thermodynamic potential for carbon deposits and the very high operating temperature limit its application. Although, it has been reported that supported noble metal catalysts (Rh, Ru, Ir, Pt and Pd) have promising catalytic performances and low sensitivities to carbon deposits, the unavailability of noble metals limits their utilization in large-scale processes. Ni is more promising than noble metals for industrial utilization [3]. Most of the studies to date on Ni-based catalysts have been carried out using alumina or silica supports [4]. Al-Ubaid and Wolf [5] found a much greater stability for Ni supported on the aluminate than on other supports. There are two major reasons for coke formation, i.e. methane decomposition and CO disproportionation. Methane decomposition is favored at high temperature and low pressure, whereas CO disproportionation is favored at low temperature and high pressure [2,6]. Rostrup-Nielsen [7] showed that carbon nucleation requires nickel ensembles of a certain size, and its aggregation will be much slower and lower rates of coke formation than it can be expected if the metal is stabilized.

The formation of aluminum spinel compounds from the parent oxides have been extensively studied in the sixties and seventies [8,9]. Up to now, a unified viewpoint on the effect of spinel formation has not emerged. The major drawbacks with these catalysts are the phase transformation e.g. the formation of $NiAl_2O_4$, their tendency to form coke deposits and the nickel sintering during reduction. In methane steam reforming it was admitted that Ni–Al_2O_3 catalysts deactivate, due to the increase of pressure drop as a result of carbon deposit and the high reaction temperatures (700–1000 K) lied to $NiAl_2O_4$, formation. Lamber and Schulz-Ekloff [10,11] showed that decoration of the nickel crystallites with $NiAl_2O_4$ is crucial for the high stability of the Ni/Al_2O_3 catalysts. Ni supported on other supports as spinel compounds: $CaAl_2O_4$ [12] or perovskite: $Ca_{0.8}Sr_{0.2}TiO_3$ [13], $BaTiO_3$ [14] and $LaNi_xFe_{1-x}O_3$ [15] presents a high activity and a better stability than Ni deposited on Al_2O_3. These structures permit a limitation of carbon formation.

---

[*] Corresponding author. Tel.: +33 3 90 24 27 69; fax: +33 3 90 24 27 68.
E-mail address: petitC@ecpm.u-strasbg.fr (C. Petit).

0920-5861/$ – see front matter © 2005 Elsevier B.V. All rights reserved.
doi:10.1016/j.cattod.2005.11.065

This paper deals with the formation of spinel by a sol–gel like method with a control of its structure and tolerance to over or sub-stoichiometry [17,18]. The reduction of NiO as a function of the initial dispersion and interaction with the spinel phase is studied by temperature-programmed reaction. Preliminary reactivity results in dry reforming of methane will be given to illustrate the interest of the catalytic preparation study.

2. Experimental

2.1. Spinel synthesis

The synthesis of well-crystallized structures close to $NiAl_2O_4$ spinel is based on the resin method from metallo-organic propionate precursors [17,18]. Nickel acetate and aluminum nitrate were used (98+ % purity, Strem) as starting salts. The salt of each metal element was separately introduced in a hot propionic acid solution until the formation of a limpid solution. Characterization in solution of the propionate species is close to those obtained for others bimetallic oxides published elsewhere [16,17]. After dissolution, the two solutions were mixed and stirred under reflux for 1 h. Propionic acid was evaporated until the formation of a resin, which hardened by cooling. Nitrate species are eliminated as a reddish-brown nitrous oxide gas during the evaporation of the propionic acid. This step occurs almost at the end of the evaporation of the solvent and is very exothermic. The obtained resins were calcined at 725, 800 or 900 °C for 4 h (heating rate of 3 $^\circ C\ min^{-1}$) and the compounds were collected once they were at a room temperature. Three Ni/Al ratios have been used during the preparation. The stoichiometric spinel $NiAl_2O_4$ presents a ratio Ni/Al equal to 0.5 corresponding to a relative atomic % of Ni equal to 33.3. These catalysts were noted S system for Spinel. According to Ni content, it is possible to determine two types of catalysts: the type with a lack of Ni and the type with an excess of Ni. The lack or excess of Ni is represented by x and is defined (in %) as $x = 100(\text{Ni content} - 33.3)/33.3$. Catalysts with an excess of Al (lack of Ni) in comparison with the spinel are denoted Al–S systems and the relative atomic percentage of Ni are tested in the range of 23.0 (Ni/Al ratio = 0.30; $x = -31\%$) to 32.1% (Ni/Al ratio = 0.47; $x = -3.6\%$). Ni/Al ratios, with an excess of Ni, are noted Ni–S systems. The relative atomic percentage of Ni are in the range of 37.0% (Ni/Al ratio = 0.59; $x = +11.1\%$) to 42.4% (Ni/Al ratio = 0.74; $x = +27.5$). Chemical analysis confirmed the expected ratios of Ni/Al in the investigated samples.

2.2. Techniques of characterization

The X-ray diffraction experiments have been performed on a D5000 Siemens diffractometer using the Cu Kα radiation ($\lambda = 0.15406$ nm). The scattering intensities were measured over an angular range of $20^\circ < 2\theta < 85^\circ$ for all the samples with a step size $\Delta(2\theta)$ of 0.03° and a count time of 2 s per step. The diffraction spectra have been indexed by comparison with the JCPDS files (Joint Committee on Powder Diffraction Standards).

The scanning electron microscopy (SEM) analysis have been performed on a JEOL JSM-840 scanning microscope equipped with an energy dispersive X-ray (EDX) device. A very thin carbon deposit was used to improve the conductivity of the sample.

Transmission electron microscopy (TEM) analysis have been performed on a TOPCON EM-002 B apparatus coupled to an energy disperse X-ray spectrometer (EDS). EDS measurements have been carried out on different areas of the samples, using a broad (200 nm diameter) or a fine (14 nm diameter) focused beam. As shown by Houalla et al. [19], the use of a fine focused beam in the scanning transmission mode for X-ray microanalysis gives information on the sample homogeneity, whereas the broad focused beam leads to the mean elemental proportions in the sample.

The BET surface area have been determined using a SA 3100 Coulter sorptometer at 77 K.

Measurements made by temperature programmed reduction were performed on a 50 mg sample placed in a U-shaped quartz reactor (6.6 mm ID) using a heating rate of 15 $^\circ C\ min^{-1}$ from 25 to 900 °C. The reductive gas used was a mixture of 3% H_2/He (total flow rate 50 $ml\ min^{-1}$). A thermal conductivity detector analyzed the effluent gas after water trapping and permitted to quantify the hydrogen consumption.

2.3. Reactivity device

Catalytic testing were performed for CO_2 reforming of methane in a tubular fixed-bed quartz reactor, at atmospheric pressure, in the temperature range 700–800 °C using 0.2 g of catalyst and a molar ratio of $CH_4/CO_2 = 1:1$ at a total flow rate of 50 $ml\ min^{-1}$ (CH_4:CO_2:Ar:N_2 5:5:35:5). The catalyst was reduced in situ at 800 °C for 2 h in a flow of 5% H_2/Ar (53 $ml\ min^{-1}$). The products and reactants are analyzed by gas chromatography. In all experiments, the performances of the catalysts were evaluated with the conversion and the yields. They are calculated as follows:

$$CH_4\ \text{conversion}\ (\%) = \frac{\text{moles of } CH_4 \text{ converted}}{\text{moles of } CH_4 \text{ in feed}} \times 100$$

$$CO_2\ \text{conversion}\ (\%) = \frac{\text{moles of } CO_2 \text{ converted}}{\text{moles of } CO_2 \text{ in feed}} \times 100$$

$$\text{yield of } H_2\ (\%) = \frac{\text{moles of } H_2 \text{ produced}}{2 \text{ moles of } CH_4 \text{ in feed}} \times 100$$

$$\text{yield of CO}\ (\%) = \frac{\text{moles of CO produced}}{\text{moles of } CH_4 \text{ in feed} + \text{moles of } CO_2 \text{ in feed}} \times 100$$

3. Results and discussion

Characterisation of the three mixtures, noted as $NiAl_2O_4$ (S system), γ-Al_2O_3/$NiAl_2O_4$ (Al–S systems) and NiO/$NiAl_2O_4$ (Ni–S system) after the preparation, are made to understand the spinel tolerance and to control the presence of free NiO.

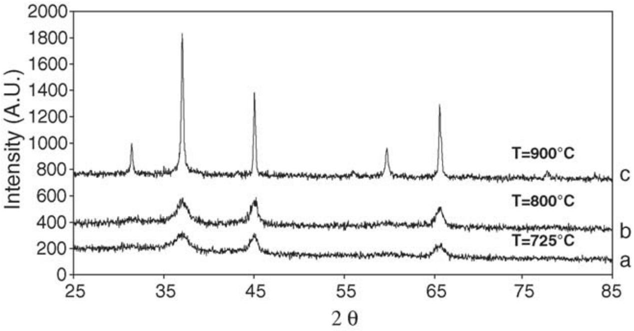

Fig. 1. X-ray analysis of S systems (stoichiometric spinel) after calcination at: (a) 725 °C, (b) 800 °C and (c) 900 °C.

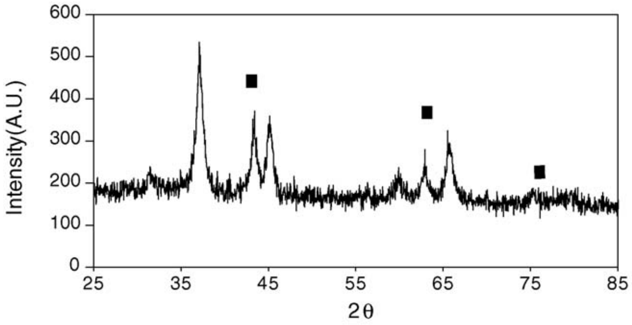

Fig. 3. X-ray spectrum of Ni–S system calcined at 900 °C (■) NiO phase.

3.1. DRX

The X-ray spectra of the S system, at different temperatures of calcination, are given in Fig. 1. For all the preparations, the diffraction analysis indicates the formation of the cubic structure of spinel. The S system spectrum fits well that of $NiAl_2O_4$ synthesized by co-precipitation and calcined at 1300 °C (JCPDS file no. 10-0339) [20]. The S system is crystallized by calcination higher than 725 °C, showing the good effect of the salt solubility in propionic acid. The crystallization of the solids increases with increasing the calcination temperature or time, as shown by the sharp peaks in Fig. 1c. The lattice parameter value for $NiAl_2O_4$ obtained at 900 °C ($a_0 = 0.8046$ nm) coincides with that reported in the literature for the same spinel prepared by the ceramic method at high temperature [21] and by the sol–gel method at 900 °C [22].

The X-ray spectrum of the 900 °C Al–S system is given in Fig. 2. For all sub-stoichiometric catalysts, the diffraction analysis indicates the formation of the spinel structure only. The crystallinity of the spinel phases also decreased. The relative ratios between the peaks are modified compared to the simple spinel phase in this case. This X-ray diffraction pattern is similar to those obtained by Otero Arean et al. [22] for 900 °C calcined sub-stoichiometric gel of Ni/Al ratio equals to 1:8. They noted that decreasing Ni/Al ratio in the samples led to the corresponding a_0 values decrease from 804.6 to 800.8 pm. Presence of alumina produces in all cases the same effect as shown by XRD profiles ((3 1 1) at 37°, (4 0 0) at 45°, (5 1 1) and (5 3 3) at 60°, (4 4 0) at 66°). The absence of diffraction lines, not ascribed to a spinel-type phase, provides a strong evidence for a solid solution formation between Al_2O_3 and $NiAl_2O_4$. It is known that the limit phase γ-Al_2O_3 dissolves (in all proportions) in many spinel-type aluminates [23].

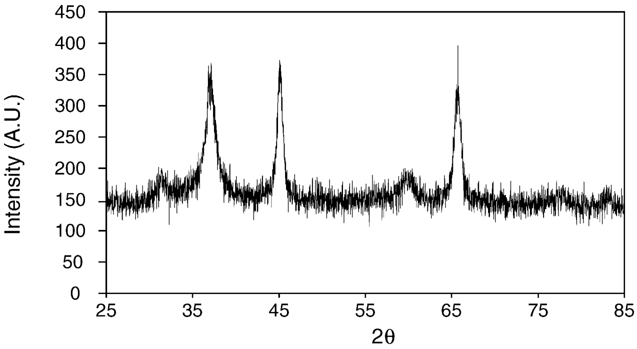

Fig. 2. X-ray spectrum of Al–S system calcined at 900 °C.

The X-ray spectrum of the 900 °C Ni–S system is given in Fig. 3. For all catalysts prepared with an excess of Ni (from 11.1% to 27.5%), the diffraction analysis indicates the formation of both spinel and NiO ($2\theta = 44.2$, 51.8 and 76.2) phases. The presence of NiO led to a decrease of crystallinity of the spinel phase as indicated by the broad XRD peaks obtained (compared to Fig. 1a).

3.2. BET

The BET surface areas of the S systems, at different temperature, are reported in Table 1. The surface areas decrease strongly between 800 and 900 °C. this is attributed to the crystallization, in good accordance with the X-ray analysis.

The BET surface areas of the Al–S systems, at different temperatures, are reported in Table 2. The surface area of the Al–S system is not too much sensitive to nickel deficiency. The values slowly decrease with increasing Ni deficiency for both calcination temperatures at 800 and 900 °C, ranging from 88 to 130 and 65–85 $m^2\,g^{-1}$, respectively. The Al–S system

Table 1
BET surface and porous volume for S system at different temperatures

Temperature of calcination (°C)	BET surface ($m^2\,g^{-1}$)	Porous volume ($cm^3\,g^{-1}$)
725	138	0.190
800	105	0.256
900	6	0.135

Table 2
BET surface of Al–S system in function of the relative atomic % of Ni and the corresponding lack of Ni after calcination at 800 and 900 °C

Ni (%)	Lack of Ni (%)	BET surface ($m^2\,g^{-1}$)	
		800 °C	900 °C
32.1	−3.6	121	85
29.9	−10.1	130	72
26.4	−20.6	104	80
23.0	−31.0	88	65

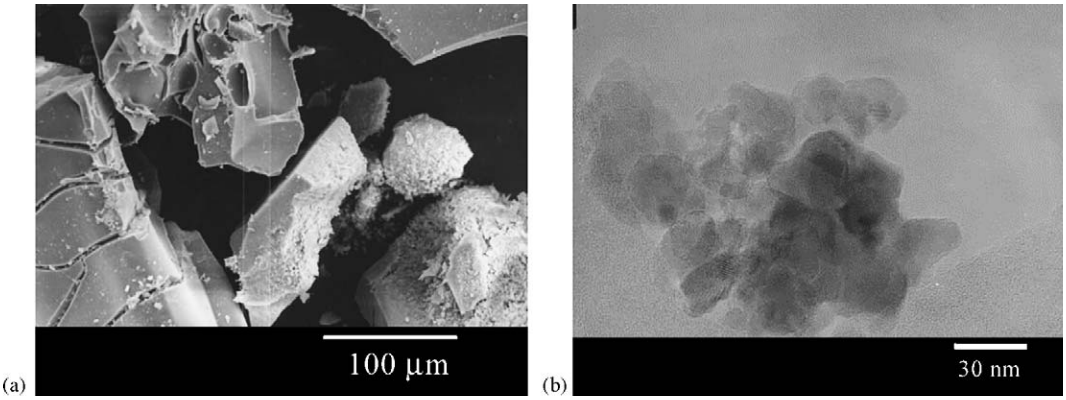

Fig. 4. (a) SEM and (b) TEM micrograph of S system calcined at 900 °C.

Table 3
BET surface of Ni–S system in function of the relative atomic % of Ni and the corresponding excess of Ni after calcination at 800 and 900 °C

Ni (%)	Excess of Ni (%)	BET surface ($m^2\ g^{-1}$)	
		800 °C	900 °C
37.0	+11.1	97	93
40.3	+20.9	95	–
42.4	+27.5	174	–

texture is mesoporous and non-well crystallized when calcined at 900 °C. It is worth noting the results obtained by Otero Arean et al. [22] showing mesoporous spinel oxides formation with higher BET surface area at 900 °C (200–290 $m^2\ g^{-1}$) when using a not conventional sol–gel method preparation.

The BET surface areas of the Ni–S systems at different Ni composition and calcination temperature are given in Table 3. The BET surface area slightly decreases with the excess of Ni from 97 to 74 $m^2\ g^{-1}$. The analysis of the pore distribution shown that those Ni–S systems present also a mesoporous texture.

3.3. SEM and TEM

The 900 °C S system shows a compact and smooth structure with some areas with granular surface as reported in Fig. 4a. Homogeneous and well defined spherical particles of 20–30 nm in size are evidenced by TEM (Fig. 4b). The micrographs show the regular succession of the atomic planes corresponding to the different planes of the $NiAl_2O_4$ lattice.

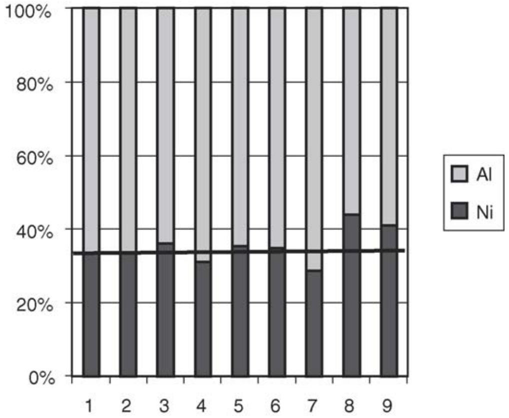

Fig. 5. EDS distribution of Ni and Al in function of the different zones of the S system calcined at 900 °C: (1) elemental analysis, (2) large beam, (3–9) fine beam.

The sample EDS analysis is presented in Fig. 5. The data, obtained with a broad focused beam, (Fig. 5, No. 2) are in close agreement with that obtained by elemental analysis (Fig. 5, No. 1) for Ni/Al ratio of 36/64. The homogeneity of the system was confirmed by EDS measurements using fine focused beam. Indeed, it was found that the main part of the S system

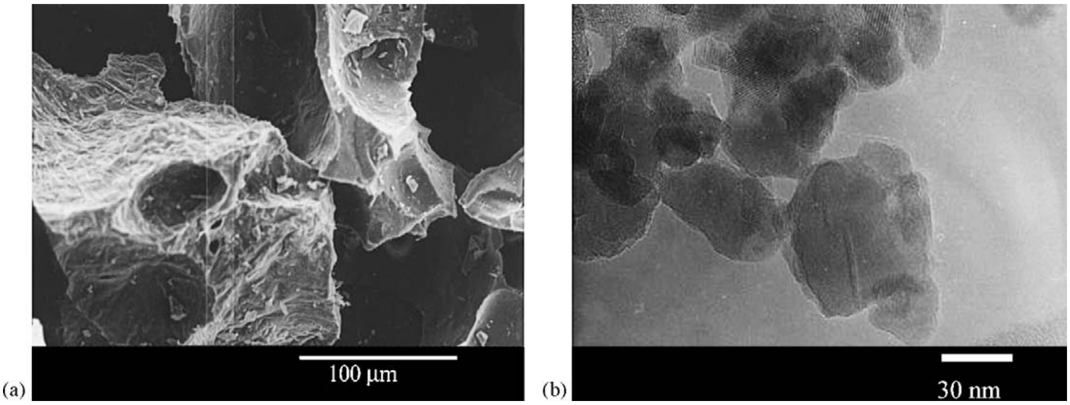

Fig. 6. (a) SEM and (b) TEM micrograph of Al–S system calcined at 900 °C.

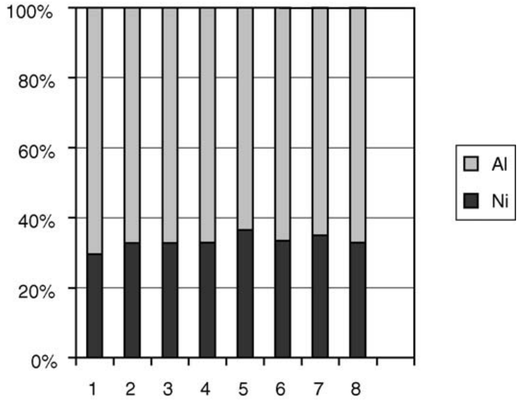

Fig. 7. EDS distribution of Ni and Al in function of the zones of the Al–S ystem calcined at 900 °C: (1) elemental analysis, (2) large beam, (3–9) fine beam.

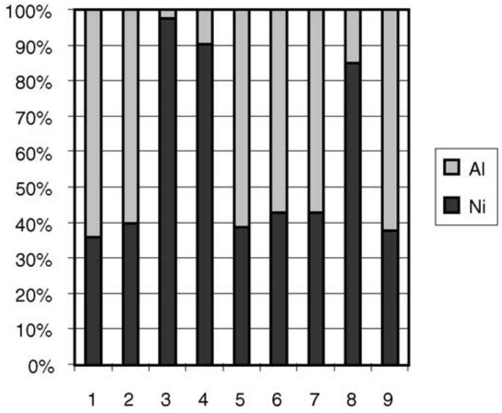

Fig. 9. EDS distribution of Ni and Al in function of the zones of the Ni–S system calcined at 900 °C: (1) elemental analysis, (2) large beam, (3–9) fine beam.

corresponds to pure spinel phase, according to the distribution of Ni and Al. Some areas present a small excess of Ni identified by dark zones in the micrographs and high amount of nickel in EDS indicated that $NiAl_2O_4$ phase is very sensitive to the relative amount of Ni and Al.

Al–S system with 10.1% deficiency in Ni and obtained at 900 °C exhibited similar morphology as the S system, as shown in Fig. 6. The Al–S systems are stringier on the surface than $NiAl_2O_4$ (Fig. 4a). Spherical spinel particles with good homogeneity in size are evidenced by TEM (Fig. 6b). Fewer large grains are observed due to agglomeration of particles. Sample EDS distribution of Ni and Al is given in Fig. 7. The high homogeneity of the Al–S system is confirmed by the constant local elemental distribution given by the EDS fine focused beam.

SEM and TEM micrographs of 900 °C Ni–S system are given on Fig. 8. The general aspect is almost the same than the spinel but the entire surface of the sample presents a granular aspect. TEM micrographs showed particles of spinel and NiO as darker and larger areas as shown on S system. These observations are confirmed by EDS analysis presented in Fig. 9.

In conclusion, evident differences are noticed on SEM micrographs between the bordering systems. In all cases, micrographs show large holes, corresponding to CO_2 or NO_2 release during the resin calcination. Mimani [24] demonstrated the significant role of the salt nature in changing the microstructure. In our case, the major effect was due to the exothermic NO_2 release.

3.4. TPR

Numerous authors reported that the active species in partial oxidation of methane are the reduced metal present at the surface of the catalyst [25]. On NiO/Al_2O_3, the reduction from free NiO to metallic nickel is studied by Swann et al. [26]. NiO was reduced at a relatively low temperature (lower than 450 °C). The temperature programmed reduction (TPR) is able to give the number of species and a relative classification of the energy bonds between the reducible element and its environment. More the element is stabilized; more the reduction temperature is high in TPR. The curves of the different S, Ni–S and Al–S systems, calcined at 900 °C, are given in Fig. 10. It must be noticed that the effect of the Ni/Al ratio is very important for the reduction of NiO [27]. In each case, reduction leads to metallic nickel deposited on γ-Al_2O_3 as determined by XRD. The S system presents mainly one reduction peak at 800 °C. This value corresponds to the stoichiometric spinel $NiAl_2O_4$ proposed in the literature. A small shoulder at 450 °C is observed and is attributed to free NiO. This point is confirmed by the EDS observation. The Al–S system presents a high-

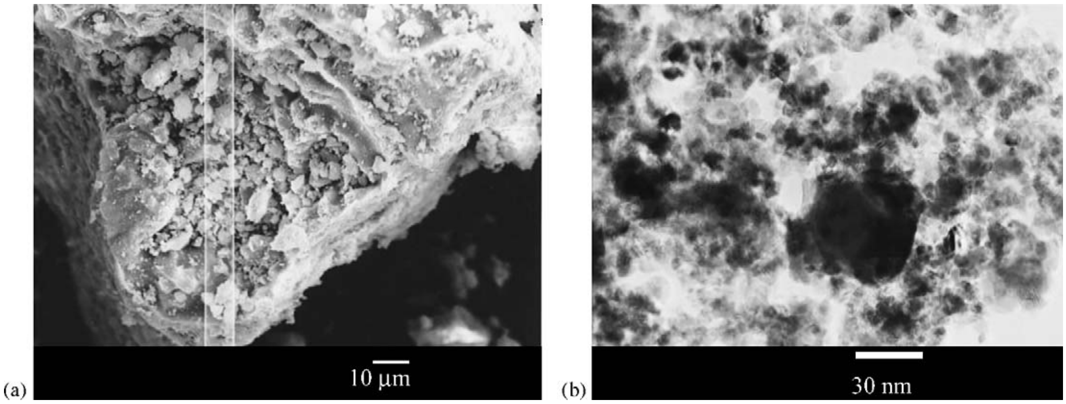

Fig. 8. (a) SEM and (b) TEM micrograph of the Ni–S system calcined at 900 °C.

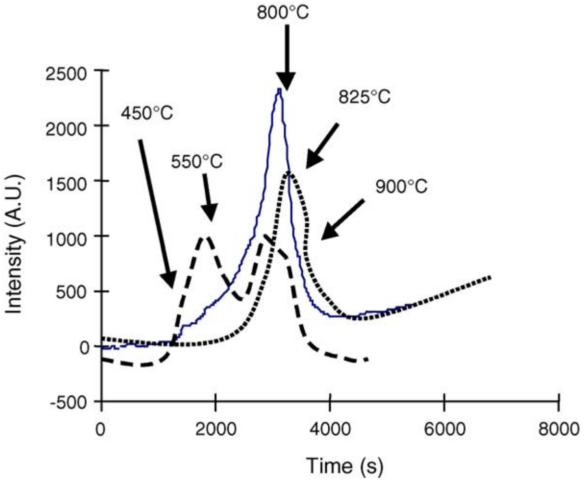

Fig. 10. Temperature programmed reduction curves of S system (—), Al–S, Ni −10.1% system (· · ·) and Ni–S system, Ni 11.1% (- - -). T calcinations, 900 °C.

defined peak of reduction at 825 °C. An excess of Al in the preparation leads to Al_2O_3–$NiAl_2O_4$ solid solution with few changes for the reduction compared to the stoichiometric phase.

The Ni–S systems present two reduction peaks. The first one at 450 °C corresponds to the reduction of the excess of NiO. Its reduction to metallic nickel helps the reduction of the nickel oxide linked into the structure. A second part is reduced at 550 °C and a third at 800 °C during the increase of temperature. The free NiO included into the $NiAl_2O_4$ phase is formed by a well-crystallized phase with small interactions with the spinel phase. It must be noted that $NiAl_2O_4$ phase is very sensitive to the Ni/Al ratio.

4. Reactivity tests

Yields of CO versus temperature give an approach of the activity of the three catalysts. At 800 °C, yields are similar (Fig. 11). However at low temperature, activity is significantly different: Ni–S catalyst is active at 450 °C, when S and Al–S only start, respectively, around 520 and 575 °C. This point could be related to the excess or default of Ni consequently to the start of reducibility of nickel of the systems: <450, 500 and ~600 °C for Ni–S, S and Al–S, respectively.

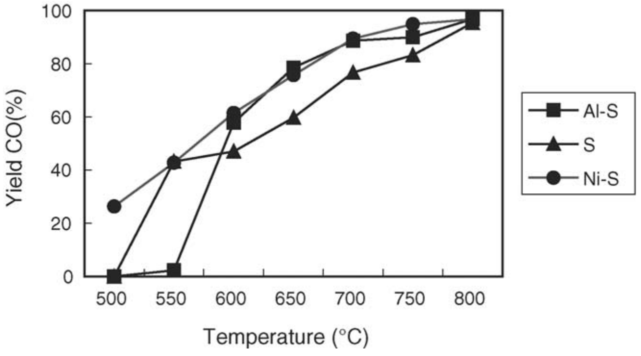

Fig. 11. Yield of CO as a function of temperature. CH_4/CO_2 = 1:1; total flow rate = 50 ml min^{-1} (CH_4:CO_2:Ar:N_2 5:5:35:5).

The CO_2 activation can be evoked via the carbonate formations as proposed in [28]. We can indicate that, by TPD of CO_2, CO_2 is not obtained around 800 °C (no carbonate decomposition). CO_2 desorbs between 300 and 500 °C with the three spinels structure. The H_2/CO ratio is <1 (~0.90) for the three spinels indicating a consumption of H_2 through reverse water gas shift reaction (RWGSR). At working temperature (800 °C) activity of the three spinels are comparable during the first part of the tests. However, the free nickel, not in strong interaction with the structure Ni–S gives, a rapid deactivation by carbon formation. For Al–S, 0.67% of the carbon coming from CH_4 or CO_2 has been transformed into carbon (mainly nanotubes) after 24 h of reactivity compared to 1.16% for S and 2.20% for Ni–S illustrating the interest of the study on the stoichiometry of the spinels.

5. Conclusion

According to the characterization of the sub, over and stoechiometric spinel structures, the sol–gel like method with propionic acid as solvent permits the formation of systems close to $NiAl_2O_4$ after calcination at 725 °C or higher. The spinel structure is a non-tolerant structure concerning an excess of Ni. If Ni/Al is higher than 0.5, free NiO is present on spinel and favors the reduction of nickel at low temperature. Stoechiometric spinel seems difficult to obtain as pure phase and forms easily small zones of free nickel oxide. If the Ni/Al ratio is lower than 0.5, a solid solution of Al_2O_3 and $NiAl_2O_4$ is formed and high surface area is obtained. To get good performance of the reforming of methane into synthetic gas with limited coke formation, small metallic particles must been obtained. The growing of the Ni particles needs to be limited. The sub-stoechiometric spinel structures present the properties to be an active catalyst: stability of the structure at low temperature, high dispersion of NiO into the spinel, formation of Ni phase in the same temperature area than the catalytic reaction and presence of Ni oxide to limit the growing of the particles probably by formation of interaction between nickel metal out of the structure and Ni oxide of the structure. Even if in dry reforming of methane same activity has been obtained during a limited time of reaction, formation of carbon is less important with the Al–S spinel illustrating the interest to study the preparation method of such compounds.

Acknowledgement

The authors are deeply grateful to M.G. Ehret for TEM experiments and for discussion.

References

[1] A.T. Ashcroft, A.K. Cheetham, J.S. Foord, M.L.H. Green, C.P. Grey, A.J. Murreill, P.D.F. Vernon, Nature 344 (1990) 319.
[2] D. Dissanayake, M.P. Rosynek, K.C.C. Kharas, J.H. Lunsford, J. Catal. 132 (1991) 117.
[3] R. Jin, Y. Chen, W. Li, W. Cui, Y. Ji, C. Yu, Y. Jiang, Appl. Catal. A 201 (2000) 71.
[4] O. Dewaele, G.F. Froment, J. Catal. 184 (1999) 49.

[5] A. Al-Ubaid, E.E. Wolf, Appl. Catal. 40 (1988) 73.

[6] S.S. Bharadwaj, L.D. Schmidt, J. Catal. 146 (1994) 11.

[7] J. Rostrup-Nielsen, J. Catal. 85 (1984) 31.

[8] F.S. Pettit, E.H. Randklev, E.J. Felten, J. Am. Ceram. Soc. 49 (1966) 199.

[9] K. Hirota, W. Komatsu, J. Am. Ceram. Soc. 60 (1977) 105.

[10] R. Lamber, G. Schulz-Ekloff, J. Catal. 146 (1994) 601.

[11] R. Lamber, G. Schulz-Ekloff, Surf. Sci. 258 (1991) 107.

[12] Y. Lu, Y. Liu, S. Shen, J. Catal. 177 (1998) 386.

[13] T. Hayakawa, H. Harihara, A.G. Andersen, K. Suzuki, H. Yasude, T. Tsunoda, S. Hamakawa, A.P.E. York, Y.S. Yoon, M. Shimizu, K. Takehira, Appl. Catal. A 149 (1997) 391.

[14] T. Hayakawa, S. Suzuki, J. Nakamura, T. Uchijima, S. Hamakawa, K. Suzuki, T. Shishido, K. Takehira, Appl. Catal. A 183 (1999) 273.

[15] H. Provendier, C. Petit, C. Estournès, S. Libs, A. Kiennemann, Appl. Catal. A 180 (1999) 163.

[16] G. Sinquin, C. Petit, S. Libs, J.P. Hindermann, A. Kiennemann, Appl. Catal. B 27 (2000) 105.

[17] A.C. Roger, C. Petit, A. Kiennemann, J. Catal. 167 (1997) 447.

[18] J.L. Rehspringer, J.C. Bernier, Mater. Rec. Soc. Symp. Proc. 72 (1986) 67.

[19] M. Houalla, F. Delannay, I. Matsuurai, B. Delmon, J. Chem. Soc. Faraday 176 (1980) 2128.

[20] Nat. Bur. Standards (US) 9 (1959) 539.

[21] C. Otero Arean, C. Mas Carbonell, G. Turnes Palomino, J.B. Parra Soto, J. Catal. 148 (1994) 403.

[22] C. Otero Arean, M. Penarroya Mentruit, A.J. Lopez Lopez, J.B. Parra Soto, Colloid Surf. A 180 (2001) 253.

[23] A. Navrotsky, O.J. Wechsler, K. Geisinger, F. Seifert, J. Am. Ceram. Soc. 69 (1986) 418.

[24] J. Mimani, J. Alloys Compd. 315 (2001) 123.

[25] B.S. Liu, C.T. Au, Appl. Catal. A Gen. 244 (2003) 181.

[26] H.M. Swann, R. Rouanet, P. Widyananda, C. Mirodatos, Stud. Surf. Catal. Sci. 107 (1997) 447.

[27] L. Zhang, J. Lin, Y. Chen, J. Chem. Soc. Faraday Trans. 80 (3) (1992) 497.

[28] J.R.H. Ross, M.C.F. Steel, J. Catal. 52 (1978) 280.